

Supporting Information

A new rechargeable battery based on zinc anode and $\text{NaV}_6\text{O}_{15}$ nanorod cathode

Saiful Islam,^a Muhammad Hilmy Alfaruqi,^{a,b} Balaji Sambandam,^a Dimas Yuniarto Putro,^a Sungjin Kim,^a Jeonggeun Jo,^a Seokhun Kim,^a Vinod Mathew,^a Jaekook Kim*^a

^aDepartment of Materials Science and Engineering, Chonnam National University, 300 Yongbong-dong, Buk-gu, Gwangju, 61186, Republic of Korea.

^bDepartemen Teknik Metalurgi, Universitas Teknologi Sumbawa, Jl. Raya Olat Maras, Sumbawa, Nusa Tenggara Barat, 84371, Indonesia.

Experimental Method

Nanorod $\text{NaV}_6\text{O}_{15}$ was prepared using a simple sol-gel method. In brief, 3 mM V_2O_5 (98%, Sigma Aldrich), 1.5 mM sodium oxalate (99.5%, Sigma Aldrich), and 9 mM oxalic acid was dissolved in 20 ml distilled water and stirred for 2 h at 50 °C until the solution turned into blue color. Thereafter, the solution was dried at 80 °C for 24 h in a pre-heated oven to obtain a dried product. The final powders were obtained after the dried powder was ground well and separated into three portions before annealing at 300 and 400 °C, respectively for 5 h in air.

The XRD analyses were performed using X'Pert PANalytical Model high-resolution X-ray diffractometer with Cu $K\alpha$ radiation ($\lambda = 1.54056 \text{ \AA}$). The prepared powder was ground well before X-ray diffraction measurement. The XRD patterns were recorded within the 2θ range from 10 to 80 at 40 kV and 30 mA. The morphology of NVO compounds were studied by field-emission scanning electron microscopy (FE-SEM) and transmission electron microscopy (TEM) techniques recorded using S-4700 Hitachi model and Philips Tecnai F20 model operating at 200 keV, KBSI, respectively. X-ray photoelectron spectroscopy (XPS) was measured by using a Multilab 2000 model (Thermo VG Scientific Instrument). Al $K\alpha$ was used as an X-ray source and the spectrometer was calibrated with respect to the C 1s peak binding energy of 284.6 eV.

In-situ XRD measurement was done using synchrotron beamline at 5A KIST-PAL (Pohang Accelerator Laboratory). High energy 2.5G eV with 200 mA current was employed to record XRD patterns at 1.00076 Å wavelength and was re-plotted with respect to the λ -value of 1.5414 Å. Furthermore, synchrotron X-ray absorption spectroscopy (XAS) technique at the BL7D beamline of Pohang light Source (PLS) in high energy 2.5 GeV with around 200 mA current condition was used to measure the ex-situ NVO sample. The collected data was converted using ATHENA software.

The cathode was prepared by mixing active material (NVO), Ketjen black, and teflonized acetylene black (TAB) as a binder, in the ratio of 70:20:10, respectively, and pasted onto stainless steel. Then, the paste was dried overnight in an oven that was pre-heated at 120 °C. The active mass loading of the NVO cathode was 3 mg. A 2032-type coin cell was assembled by placing glass fiber between cathode and Zn metal anode. 1M ZnSO_4 aqueous solution was used as electrolyte.

The prepared coin cell was aged for 12 h before checking the galvanostatic electrochemical reaction. Electrochemical measurement was performed using BTS 2004H model (NAGANO) battery tester at different test conditions within the potential range 1.4 to 0.4 V vs. Zn/Zn²⁺. AUTOLAB PGSTAT302N was used to perform the cyclic voltammetry (CV) analysis. Electrochemical impedance (EIS) of Zn/NVO was recorded with the range 100 mHz to 10 kHz by using BTS 2004H (Nagano) analyzer.

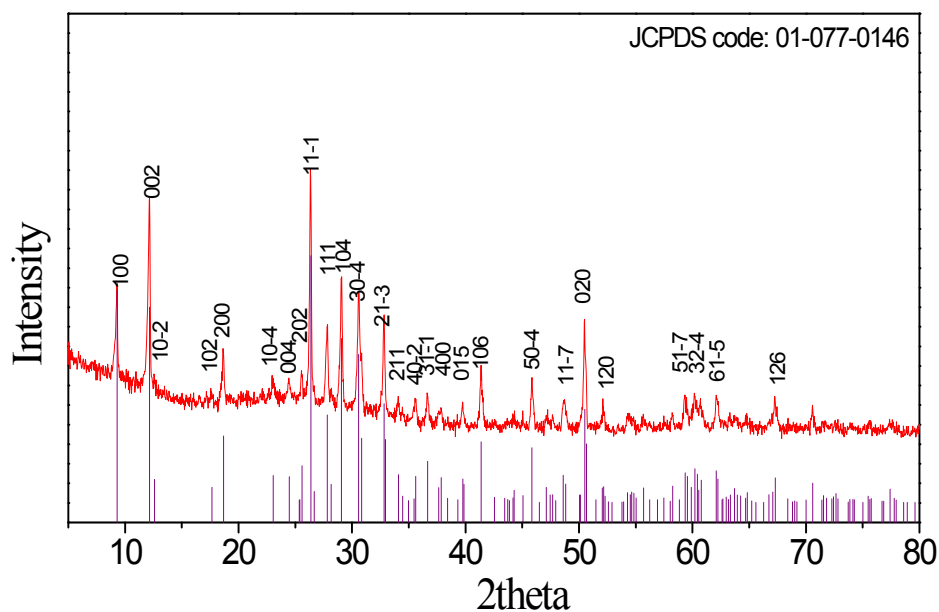


Figure S1 XRD pattern of the NVO-400 sample.

XRD pattern of the NVO-400 sample indicates that the crystallinity of the sample improved with increasing temperature. In this case, the phase remains unchanged.

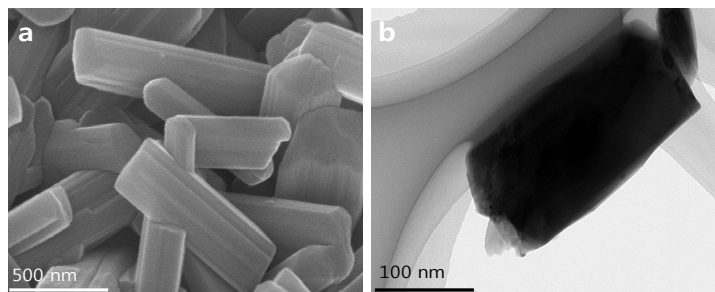


Figure S2 (a) FE-SEM and (b) TEM images for the NVO-400 sample.

The NVO-400 samples display an average length of 300 and 500 nm, respectively. The SEM and TEM results suggest that the particle size increases as the temperature increases.

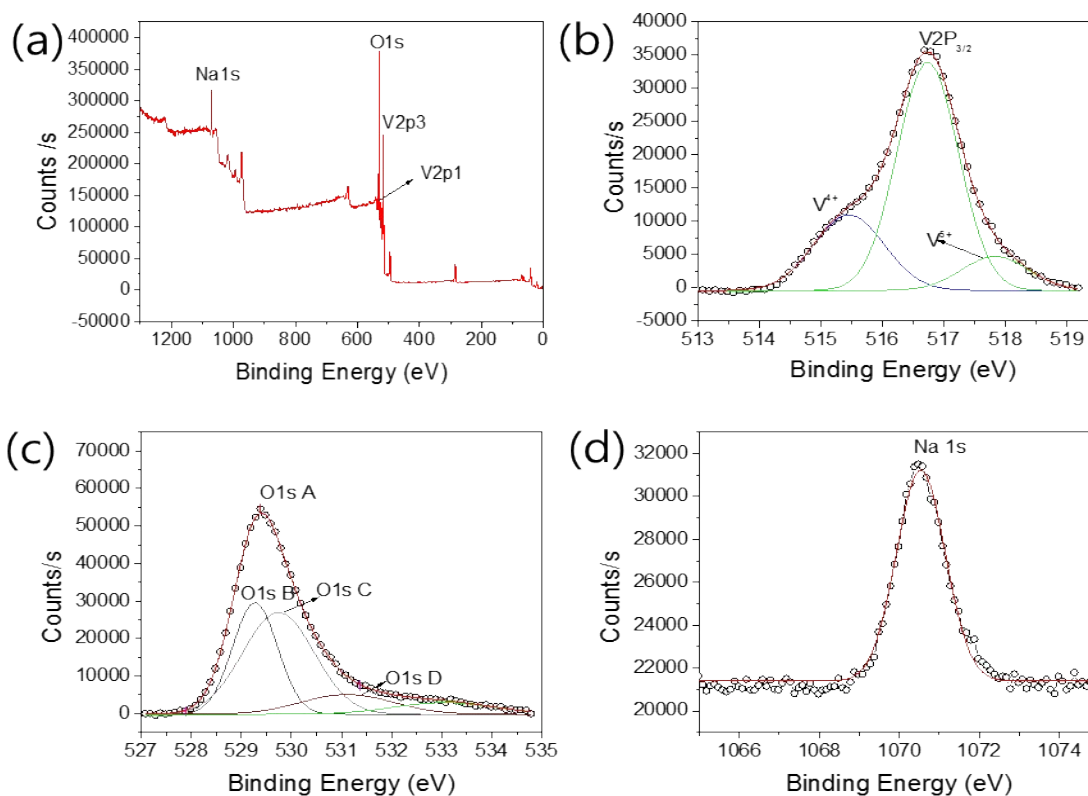


Figure S3 Wide scan XPS spectra of (a) NVO-300 sample and corresponding narrow scan (b) vanadium, (c) oxygen, and (d) sodium elements.

The texture composition was further clarified through XPS analysis for the NVO-300 sample. Fig. S3a shows the survey scan with notable elemental positions. The deconvoluted V 2p profile in Fig. S3b representing the oxidation state of V^{4+} , V^{5+} and its satellite shoulder peaks stand at 515.4, 516.7 and 517.8 eV, respectively. The origin of V^{4+} and V^{5+} with predominant character of the latter oxidation state thus confirm the overall oxidation state is close to 5+. Similarly, the binding energy at 528.39 eV is attributed to O 1s (Fig. S3c). A clear profile for Na 1s peak observed at 1070.5 eV, confirms the Na^+ identity (Fig. S3d).¹

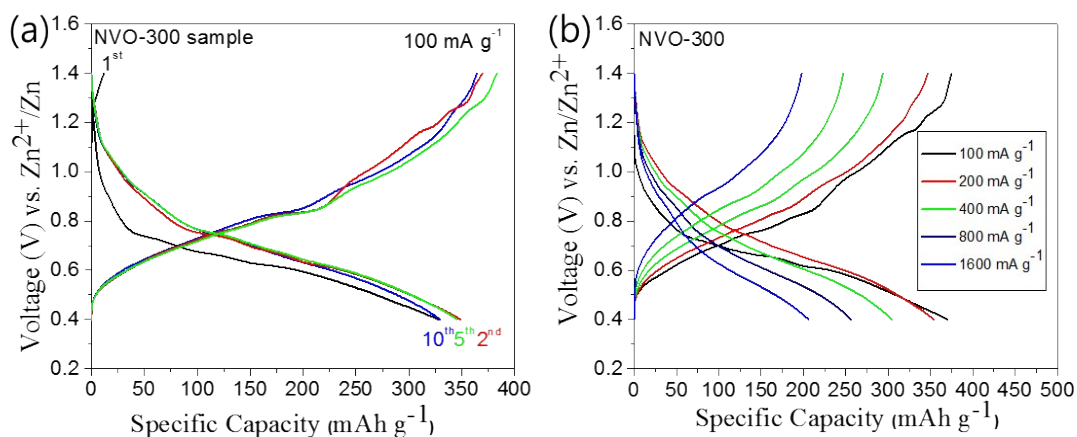


Figure S4 Electrochemical charge-discharge curve of NVO-300 sample within potential window 0.4 to 1.40 V at (a) 100 mA g⁻¹ and (b) at 100, 200, 400, 800 and 1600 mA g⁻¹ current densities.

Generally, sodium ion extraction from vanadium-based crystalline hosts like $Na_3V_2(PO_4)_3@C$ in aqueous electrolytes occur at a higher charging potential (~ 1.58 V).² For further clarification, we performed the electrochemical measurement of the present NVO-300 sample by initially charging the electrode at 100 mA g⁻¹ until 1.40 V and the resulting profile revealed no feature corresponding to Na^+ extraction (Fig. S4). The observation thus confirmed that sodium ions are not extracted from the layered structure of the present NVO during electrochemical charging. In addition, we also performed ICP analysis for the discharge cathode and electrolyte (Table S1). ICP

analysis confirms that the presence of Na in the discharge electrode, while in the discharge electrolyte only negligible amount of Na could be traced. This supports Zn intercalation into the cathode as well as suggests that Na remains in the cathode and no Na leaching upon electrochemical reaction.

Table S1 *Ex-situ* ICP analyses of the discharge electrode and electrolyte.

| Sample | Element | Concentration (ppm) |
|-----------------------|---------|---------------------|
| Discharged Electrode | Na | 143 |
| | Zn | 251 |
| Discharge Electrolyte | Na | 4 |

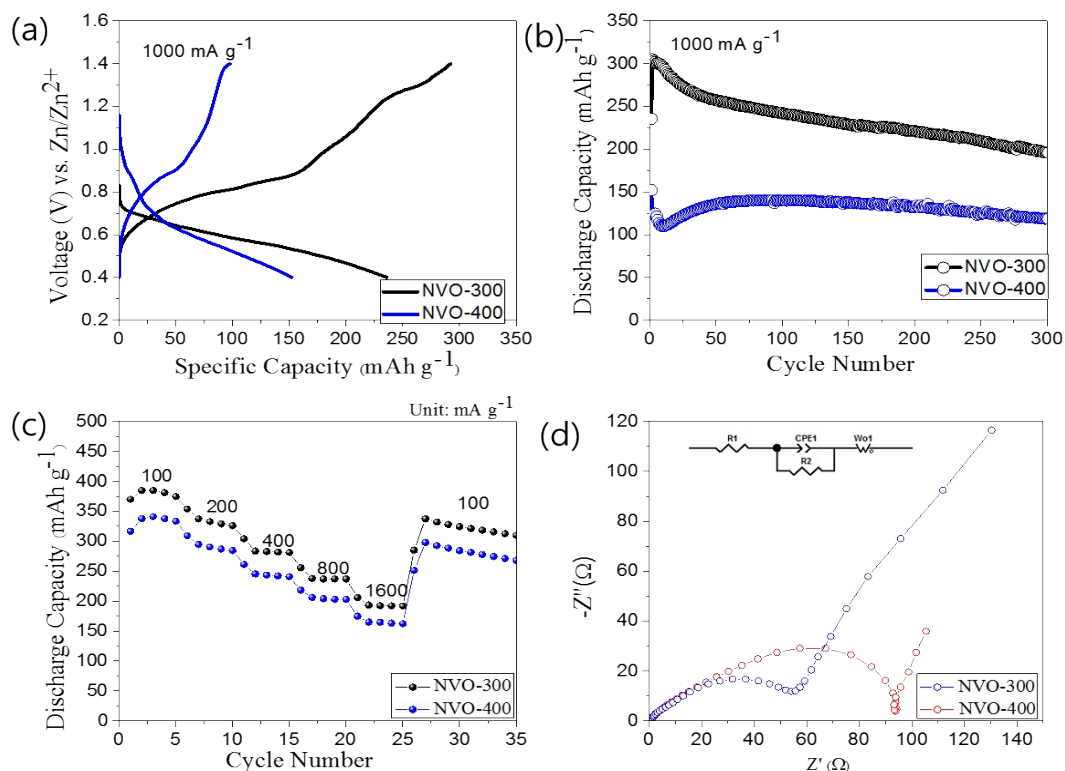


Figure S5 Comparison of electrochemical performance of the NVO-300 and NVO-400 samples. (a) ECD pattern at 1000 mA g⁻¹, (b) cycle life at 1000 mA g⁻¹, (c) rate capability and (d) Nyquist plots of the Zn/NVO-300 and Zn/NVO-400 cells.

Fig. S5a displays the galvanostatic electrochemical initial charge/discharge patterns for the different samples at a high current density of 1000 mA g^{-1} . The initial discharge capacities of 235 and 152 mAh g^{-1} , were noted, respectively, for NVO-300 and NVO-400 electrodes. Long-term cyclability measurements were performed to investigate the superior electrochemical performances of NVO-300 compared to NVO-400 electrodes under a similar current density condition of 1000 mA g^{-1} . It can be seen from Fig. S5b that the NVO-300 sample delivered a high discharge capacity of 195 mAh g^{-1} after 300 cycles, while the NVO-400 sample showed less a capacity of 118 mAh g^{-1} . Rate capability test also showed that the NVO-300 sample displays superior performance. From Fig. S5c, the NVO-400 electrodes registered 316 mAh g^{-1} discharge capacities at 100 mA g^{-1} current density, respectively. Under the same electrochemical conditions, NVO-300 delivered 370 mAh g^{-1} specific capacity, which is nearly more than 17% of the capacities achieved by the electrodes prepared at higher temperature. Interestingly, at 1600 mA g^{-1} current rate, the average discharge capacities of NVO-300, NVO-400 were 195, and 166 mAh g^{-1} , respectively. After cycling at high current densities, the NVO-300 recovered to 285 mAh g^{-1} at 100 mA g^{-1} whereas NVO-400 restores only 251 mAh g^{-1} capacities.

For further clarification, electrochemical impedance spectroscopy (EIS) was employed for all electrodes (before cycling) and the results are displayed in Fig. 5d. The equivalent circuit is given in inset, here R1 stands for series resistance (R_s), R2 indicates charge transfer resistance (R_{ct}) between electrolyte/electrode interfaces, CPE represents constant phase element and W_o represents the Warburg element. The observed charge transfer resistance, R_{ct} , for NVO-300 and NVO-400 were 50 and 93Ω , respectively. As expected, the lowest R_{ct} value endows the high performance of the electrode. The results of impedance study well match with the corresponding galvanostatic electrochemical performances.

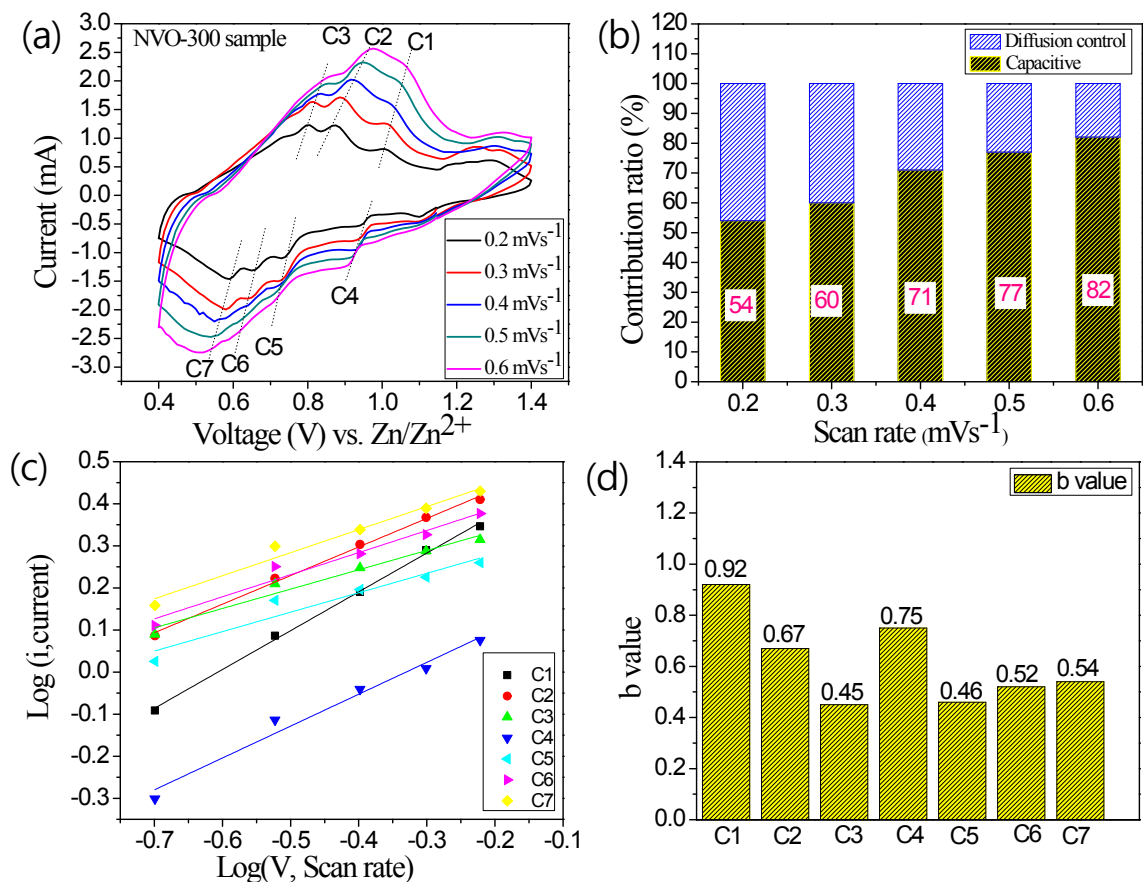


Figure S6 (a) CV curve at different scan rate. (b) Capacity contribution ratios vs. scan rates plot. (c) log(i) vs. log (V, scan rate) plots of the cathodic current response at seven peaks shown in (a) and (d) the calculated b value of the different redox peak obtained from (c) curve.

Following equation employed to perform electrochemical kinetics of NVO-300 sample:

$$i = av^b \quad (1)$$

where i is current, v is scan rate, and a and b are adjustable parameters. Here the peak C1 to C7 are taken for analysis (Fig. S6a). The b value calculated from the slope of the log (i) vs. log (v) plot in Fig. S6c. As shown in Fig. S6d, the b values of peaks C1-C7 are observed to be 0.92, 0.67, 0.45, 0.75, 0.46, 0.52, 0.54, indicating mostly capacitor like kinetics (surface controlled capacity), as commonly observed in the vanadium-based cathodes.³⁻⁵

References

1. H. He, X. Zeng, H. Wang, N. Chen, D. Sun, Y. Tang, X. Huang and Y. Pan, *J. Electrochem. Soc.*, 2014, **162**, A39–A43.
2. S. Islam, M. H. Alfaruqi, D. Y. Putro, V. Mathew, S. Kim, J. Jo, S. Kim, Y.-K. Sun, K. Kim and J. Kim, *ChemSusChem*, 2018, **11**, 2239–2247.
3. J. Ding, Z. Du, L. Gu, B. li, L. Wang, S. Wang, Y. Gong, S. Yang, *Adv. Mater.*, 2018, **30**, 1800762.
4. X. Dong, L. Chen, J. Liu, S. Haller, Y. Wang, Y. Xia, *Sci. Adv.*, 2016, **2**, e1501038.
5. Y. Yang, Y. Tang, G. Fang, L. Shan, J. Guo, W. Zhang, C. Wang, I. Wang, J. Zhou, S. Liang, *Energy Environ. Sci.*, 2018, **11**, 3157.